European Organisation for Astronomical Research in the Southern Hemisphere
Observing Programmes Office • Karl-Schwarzschild-Strasse 2 • D-85748 Garching bei München • email: opo@eso.org • Tel: +49 89 3200 6473

Received by ESO Observing Programmes Office

Cycle: P113
Type: Normal
Status: Valid
Printed: 29 Jan 2026

APPLICATION FOR OBSERVING TIME **113.26FT**

IMPORTANT NOTICE

An ATLAS view on the occurrence of core-collapse supernovae as a function of metallicity

ABSTRACT

Recently, observations have suggested that the occurrence of core-collapse supernovae (CCSNe) is strongly dependent on environment metallicity, with more CCSNe exploding at low metallicity environments. Given the importance of this result to many areas of astrophysics (as it affects our understanding of CCSN explosions, star-formation across galaxies and how the initial mass function (IMF) changes with environment properties), verification is required with distinct SN samples. We request MUSE observations of 95 host galaxies of ATLAS discovered CCSNe to robustly check the possible metallicity effect on the occurrence of these events. The analysis of a new sample will provide results independent of previous survey biases and substantially increase the statistical significance. Additionally, these observations will directly test model predictions of dust evolution, IMF, and delay time distributions of CCSNe across the Universe.

SCIENTIFIC KEYWORDS

stars: supernovae, galaxies: abundances, stars: evolution

RUNS

Run	Period	Instrument	Tel. Setup	Constraints	Mode	Type	Propr. Time	Time Constr.	Req. Time
113.26FT.001 • Run 1	113	MUSE	UT4	FLI: 100% • Turb.: 85% • pwv: 30.0mm • Sky: Variable, thin cirrus	SM	Normal	12m	✕	99h00m

AWARDED AND FUTURE TIME REQUESTS

Time already awarded to this project

Instrument	Time	Comment
MUSE	60h	111.24UM. SM. Current semester, 78% completed, data to be analyzed.
MUSE	99h	096.D-0296(A). SM. 72% completed. All data are reduced and analysed. Published and in prep. papers.
MUSE	99h	103.D-0440(A). SM. 82% completed. All data are reduced and analysed. Published and in prep. papers.

Future time requests to complete this project

- none -

Special Remarks

This project is a ‘filler’ program, with targets across the full RA and DEC range, that are observable in THN, bad seeing conditions, and during bright time. We understand that only part of the observations may be completed.

DESCRIPTION OF THE PROPOSED PROGRAMME

A- Scientific Rationale

Core-collapse supernovae (CCSNe) are luminous explosions associated with the end of the life of massive (≥ 8 $M_\odot$) stars. These events are responsible for dramatic changes in the evolution galaxies, triggering or ceasing the formation of new stars. They are also the main formation channel of heavy elements, thus being a fundamental driver of chemical enrichment in galaxies. The study of CCSNe has, therefore, a deep impact not only on the study of stellar evolution but on many fields of astronomy.

Because most massive stars explode as CCSNe, their occurrence is directly linked to the star-formation (SF) rate across the Universe. The rate of CCSNe can therefore be used as a tracer of how SF changes with respect to physical properties, such as age and metallicity. Recently, Pessi+23 used a sample of CCSNe discovered by the All Sky Automated Survey for SuperNovae (ASAS-SN) and showed that **the occurrence of CCSNe has a strong dependence on metallicity**, with these events prefering lower metallicity regions. They show that the difference between the occurrence of CCSN per unit SF between Small Magellanic Cloud (SMC) and solar metallicities has a very large factor of ~ 15 (Fig. 1, left). Additionally, they show that the distribution of CCSN metallicity does not follow the overall SF distribution in their sample. This was an unexpected result, which disagrees with most stellar population and black hole formation models (e.g., Heger+03), and has deep implications not only for massive star evolution, but also other areas of astronomy.

Some of the possible physical reasons that explain this result are: i) **a metallicity effect on the explodability of massive stars** - this would imply that there is a larger number of massive stars exploding as CCSNe at lower metallicity environments, which has strong implications to our current understanding of the mechanism behind CCSN explosions; ii) **selection effects:** a large number of CCSN events might be missed due to intrinsic properties of the survey (to e.g., highly extincted regions) - if this is the case, current CCSN rates are being underestimated by a significant factor; iii) **a metallicity dependence on the initial mass function (IMF)** - the shape of the IMF could be such that it is producing more massive stars per unit SF at low metallicity. This would be strong evidence for a dependence of the IMF on environment properties; iv) **The Hα ionization is significantly biased towards massive SF** - this would imply that the Hα to star-formation rate (SFR) conversion is significantly affected by metallicity, and that current stellar evolution prescriptions are underestimating this effect by a large factor. Because of the high impact of these results to many fields of astrophysiscs, affecting our understanding of SF and IMF across different properties of galaxies, **the metallicity dependence on the occurrence of CCSNe should be tested by new samples.**

We propose to observe CCSN host galaxies discovered by the Asteroid Terrestrial-impact Last Alert System (ATLAS) survey (Tonry+18). ATLAS is a recent all-sky high-cadence transient survey dedicated to monitoring small bodies in the solar system. Because it is a panoramic and untargeted survey, it also discovers SNe (and other extragalactic transients) homogeneously. We plan to use the volume-limited ATLAS 100 Mpc sample, which will allow us to test the metallicity dependence on the occurrence of CCSNe with different survey biases than previous studies. Additionally, ATLAS can discover and follow up fainter SNe ($m < 19$ mag) than ASAS-SN ($V < 17$ mag), being more complete in terms of luminosity function, and allowing for a smaller bias towards brighter events. Finally, ATLAS has high-cadence optical transient light-curves (LCs), which allows for a more complete selection and analyses of SN sub-types.

B- Immediate Objective

We propose MUSE observations of **95 ATLAS CCSN host galaxies (70 II, 7 Ic, 8 Ib, 6 IIb, 2 Ib/c, and 1 Ic-BL).** These targets were randomly selected from all galaxies that hosted CCSNe detected by the ATLAS survey between 2017 September and 2021 March, up to a distance of 100 Mpc, that have a classification spectrum, below a declination of $+30°$, and with no previous MUSE observations. The number of selected galaxies was defined by the time limit of a normal programme (99h), with a total of 1h per target and with some galaxies requiring more than one pointing. The number of objects selected is also similar to the sample size of previous works (e.g., Pessi+23). MUSE is the only IFU instrument in operation that can provide at the same time exquisite spatial sampling, good wavelength coverage, and a large field of view, allowing for a very detailed characterization of CCSN host galaxies. We will use established techniques of stellar continuum fitting (with `STARLIGHT`, Cid Fernandes+11), HII regions segmentation (with `IFUanalysis`, Lyman+18 - Fig. 1, right) and emission line characterization to derive physical parameters (specially lines of Hα, Hβ, O [III], S II and N II, used to estimate age, SFR and metallicity) at a local and global scale within the galaxies. Specifically, our main goal is to:

1) Robustly check the occurrence of CCSNe as a function of metallicity. With a new and more complete (in terms of SN brightness) CCSN sample, we will be able to check the surprising results of Pessi+23 and whether the occurrence of CCSN show a clear dependence on metallicity (i.e., whether the ATLAS sample follows the same behavior as observed in Fig.1, left). These observations will provide results with distinct survey biases and increase significantly the statistics when combining the samples (e.g., with ASAS-SN). We also plan to estimate the occurrence of CCSNe as a function of other environmental parameters, such as age and extinction. Additionally, we plan to use ATLAS survey rates to compare these results to models of IMF, dust evolution, and delay time distributions of CCSNe across the Universe, which will provide important results for different fields of astrophysics.

Additional results:

These will be the first observations of ATLAS SN host galaxies with MUSE. They will significantly increase the current sample of SN host galaxies observed by the VLT and the data will be available not only for transient but other extragalactic studies. This dataset will additionally allows for a very detailed analysis of CCSN environments and produce significant results. As a product of this sample, we will additionally be able to:

2) Analyze the local environments of ATLAS CCSNe. We plan to analyze the extracted spectrum around the CCSN locations to derive physical parameters of SFR, metallicity, stellar population age, and extinction. A new large sample of CCSNe will allow us to obtain statistically significant results. We will compare the results for the different CCSN subtypes in order to constrain the age and mass ranges of their progenitor stars.

3) Look for correlations between the light curve (LC) properties of CCSNe and their environments. Important physical parameters of the explosion can be derived from the observed LCs of SNe, such as the total ejecta mass, estimated from the LC width, and the ^{56}Ni mass, estimated from the peak absolute magnitude or late-time decline. Previous results show indications for a correlation between these parameters and the physical properties of their local environments for CCSNe (e.g., Galbany+18). Because all ATLAS CCSNe within 100 Mpc have a high signal-to-noise and high-cadence photometry (being more complete than previous surveys, e.g., ASAS-SN), this analysis will provide more significant results than previous works.

Figures

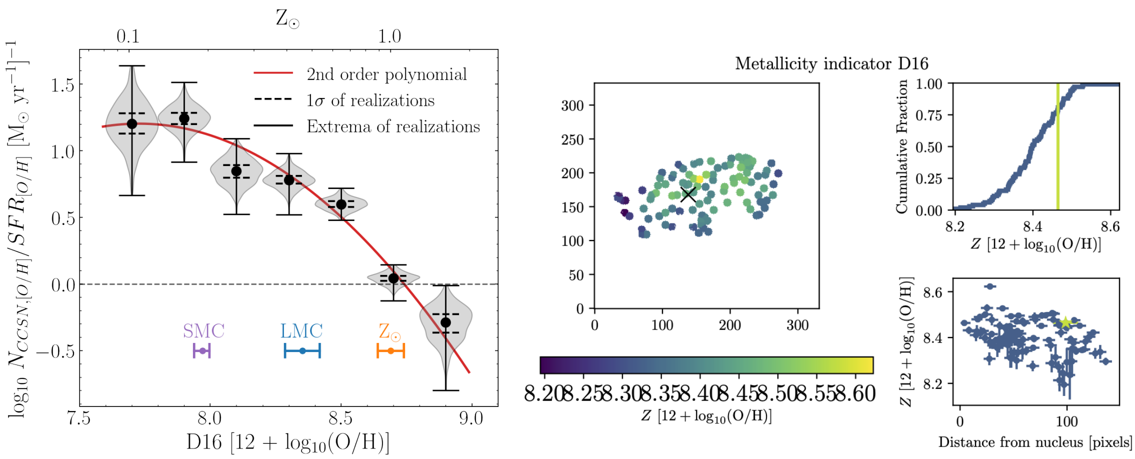

Fig. 1: *Left*: The occurrence of CCSN per unit SF as a function of metallicity derived from the ASAS-SN sample, from Pessi+23. This quantity is estimated by dividing the number of CCSNe by the total SFR over binned intervals in the metallicity axis. The plot shows a strong dependence on metallicity, with CCSNe occurring per unit SF with a much larger factor at low metallicity environments. *Right*: Output from the code `IFUanalysis` for the MUSE datacube of the galaxy IC4224, that hosted the Type II SN ATLAS17hpc. The left panel shows all the identified HII regions in the galaxy, with the colorbar showing the metallicity given by the D16 index (Dopita+16). The right top and bottom panels show, respectively, the cumulative distribution of metallicity and the metallicity gradient, obtained from these regions, with the SN position marked in green. We plan to use this code to perform HII region segmentation of the observed galaxies, in order to characterize the physical parameters obtained from the spectra of the star-forming regions across those galaxies.

References

1. Pessi, T., et al. (2023) "A metallicity dependence on the occurrence of core-collapse supernovae", arXiv, arXiv:2306.11962 – **2.** Heger, A., et al. (2003) "How Massive Single Stars End Their Life", ApJ, 591, 288 – **3.** Tonry, J. L., et al. (2018) "ATLAS: A High-cadence All-sky Survey System", PASP, 130, 064505 – **4.** Cid Fernandes, R., et al. (2011) "STARLIGHT: Spectral Synthesis Code", ascl.soft, ascl:1108.006 – **5.** Lyman, J. D., et al. (2018) "Investigating the diversity of supernovae type Iax: a MUSE and NOT spectroscopic study of their environments", MNRAS, 473, 1359 – **6.** Galbany, L. , et al. (2018) "PISCO: The PMAS/PPak Integral-field Supernova Hosts Compilation," APJ, 855, 107 – **7.** Dopita, M. A., et al. (2016) "Chemical abundances in high-redshift galaxies: a powerful new emission line diagnostic", Ap&SS, 361, 61

TARGETS

Name	RA	Dec	Coord	Runs	Comment
2020ocz	05:10:44.202	-31:35:37.522	J2000	1	SN II
V=11.9					
2019ejj	08:07:08.776	-28:03:11.642	J2000	1	SN II
V=11.9					
2018ke	13:08:39.531	-41:27:16.366	J2000	1	SN II
V=11.9					
2018ecf	14:06:34.388	-34:18:04.079	J2000	1	SN II
V=11.9					
2017izl	13:19:55.343	-47:17:05.489	J2000	1	SN II
V=11.9					
2020ad	13:57:56.805	-29:17:07.379	J2000	1	SN II
V=11.9					
2020bfb	12:54:44.220	-39:51:09.536	J2000	1	SN Ic
V=11.9					
2020admc	11:54:06.067	-39:51:52.715	J2000	1	SN Ib
V=11.9					
2020acpi	11:35:46.563	-49:02:12.257	J2000	1	SN II
V=11.9					
2021bmw	13:47:39.716	-29:25:54.620	J2000	1	SN II
V=11.9					
2018ass	21:10:19.010	-29:31:22.253	J2000	1	SN IIP
V=11.9					
2019cwt	20:00:40.210	-34:47:43.040	J2000	1	SN Ic-pec
V=11.9					
2018cmj	01:38:53.322	-42:35:22.394	J2000	1	SN II
V=11.9					
2020zae	20:07:47.943	-29:48:49.982	J2000	1	SN Ib/c
V=11.9					
2019gvp	16:46:35.511	-31:35:30.894	J2000	1	SN Ib
V=11.9					
2020mrj	14:24:24.462	-28:37:54.430	J2000	1	SN II
V=11.9					
2020voh	23:03:40.285	-36:01:40.354	J2000	1	SN II
V=11.9					
2020mvk	13:35:45.684	-30:52:30.396	J2000	1	SN II
V=11.9					
2021aez	15:36:03.959	-37:18:04.306	J2000	1	SN II
V=11.9					
2020aboq	06:38:23.738	-35:13:29.114	J2000	1	SN Ic-BL
V=11.9					
2017hhx	22:00:32.920	-27:13:29.478	J2000	1	SN IIP
V=11.9					
2017hxj	23:58:00.701	-41:32:02.706	J2000	1	SN II
V=11.9					
2018dza	14:49:17.991	-30:17:22.297	J2000	1	SN II

Name	RA	Dec	Coord	Runs	Comment
V=11.9					
2018emt	22:10:35.660	-27:14:58.697	J2000	1	SN II
V=11.9					
2019thi	11:15:15.322	-27:39:11.822	J2000	1	SN II
V=11.9					
2019xtw	02:43:33.630	-38:37:30.720	J2000	1	SN II
V=11.9					
2019axz	14:30:16.676	-43:33:41.094	J2000	1	SN II
V=11.9					
2019nyn	01:07:37.207	-41:51:12.348	J2000	1	SN II
V=11.9					
2019ofc	01:33:36.919	-38:35:59.014	J2000	1	SN II
V=11.9					
2019uhm	10:28:48.470	-31:29:52.076	J2000	1	SN II
V=11.9					
2020cnu	04:24:08.165	-27:04:47.593	J2000	1	SN II
V=11.9					
2019dna	21:05:23.801	+19:44:34.375	J2000	1	SN II
V=11.9					
2017ixz	07:47:03.056	+26:46:25.936	J2000	1	SN IIb
V=11.9					
2020obd	02:28:35.910	-10:32:18.758	J2000	1	SN II
V=11.9					
2018fy	09:53:20.020	-18:25:09.786	J2000	1	SN II
V=11.9					
2017ivh	13:39:36.252	-11:28:55.884	J2000	1	SN II
V=11.9					
2019pad	15:03:44.238	-03:17:47.080	J2000	1	SN II
V=11.9					
2019ovq	04:10:18.717	+13:24:14.875	J2000	1	SN II
V=11.9					
2018is	13:16:57.347	-16:37:04.181	J2000	1	SN II
V=11.9					
2018imj	06:51:05.759	+12:54:55.642	J2000	1	SN IIP
V=11.9					
2020fsb	15:39:03.810	-25:58:28.240	J2000	1	SN II
V=11.9					
2020abjq	01:06:14.630	+03:34:26.112	J2000	1	SN II
V=11.9					
2020qbu	01:33:53.394	-13:04:49.184	J2000	1	SN Ic
V=11.9					
2019edo	12:11:51.587	+24:08:11.753	J2000	1	SN II
V=11.9					
2017hqj	21:05:39.017	+11:24:31.784	J2000	1	SN IIP
V=11.9					
2021duv	11:45:54.636	+22:27:16.448	J2000	1	SN II
V=11.9					

Name	RA	Dec	Coord	Runs	Comment
2018hhr	02:55:48.931	+01:04:42.528	J2000	1	SN II
V=11.9					
2020mjm	14:29:29.331	-00:01:17.767	J2000	1	SN II
V=11.9					
2020nja	01:34:34.688	-03:20:37.669	J2000	1	SN II
V=11.9					
2018hjx	03:24:55.582	-02:49:19.736	J2000	1	SN Ib
V=11.9					
2020twk	23:29:13.482	-02:05:42.018	J2000	1	SN II
V=11.9					
2020njz	02:01:51.016	-10:28:11.827	J2000	1	SN Ic
V=11.9					
2019leu	19:05:16.366	+27:00:25.531	J2000	1	SN II
V=11.9					
2018ino	11:26:42.522	+20:43:37.052	J2000	1	SN II
V=11.9					
2019jyw	01:06:30.211	-02:11:56.303	J2000	1	SN II
V=11.9					
2020igs	09:36:55.416	+08:33:44.554	J2000	1	SN II
V=11.9					
2019abb	07:54:17.275	+14:16:23.257	J2000	1	SN Ic
V=11.9					
2017hpn	09:08:01.713	+27:15:04.720	J2000	1	SN IIP
V=11.9					
2018dht	20:55:19.057	+00:32:18.784	J2000	1	SN II
V=11.9					
2018hij	08:24:30.551	+18:36:15.286	J2000	1	SN IIP
V=11.9					
2017hyh	07:10:41.078	+06:27:41.281	J2000	1	SN IIb
V=11.9					
2019yc	00:39:34.990	+00:52:04.310	J2000	1	SN IIb
V=11.9					
2019gqm	19:48:09.566	-24:26:36.337	J2000	1	SN II
V=11.9					
2018cup	12:35:22.969	+29:29:31.888	J2000	1	SN II
V=11.9					
2019hqm	17:36:56.190	+21:06:17.600	J2000	1	SN II
V=11.9					
2020hop	13:19:28.193	-13:43:25.241	J2000	1	SN Ic
V=11.9					
2020zgl	23:28:01.148	-02:09:53.636	J2000	1	SN Ib-pec
V=11.9					
2017iit	05:03:20.154	+18:27:03.031	J2000	1	SN II
V=11.9					
2019sox	21:31:24.722	+02:29:39.016	J2000	1	SN II
V=11.9					
2020aqy	15:01:54.667	+25:57:59.051	J2000	1	SN II

Name	RA	Dec	Coord	Runs	Comment
V=11.9					
2019bkc	10:00:22.548	-03:01:12.558	J2000	1	SN Ic
V=11.9					
2020ovk	23:54:17.730	+26:19:36.131	J2000	1	SN II
V=11.9					
2019tsf	11:08:32.790	-10:28:54.365	J2000	1	SN Ib
V=11.9					
2020hvp	16:21:45.394	-02:17:21.322	J2000	1	SN Ib
V=11.9					
2018fer	20:33:05.235	-20:51:24.390	J2000	1	SN IIb
V=11.9					
2019dtt	22:34:37.507	+00:10:32.628	J2000	1	SN II
V=11.9					
2019aax	12:17:05.658	-26:37:44.620	J2000	1	SN II
V=11.9					
2018bvi	14:14:18.412	+10:40:41.722	J2000	1	SN Ib
V=11.9					
2018ub	11:54:58.712	+06:19:47.294	J2000	1	SN II
V=11.9					
2018fcx	04:05:56.717	-15:08:43.595	J2000	1	SN IIb
V=11.9					
2020pub	10:37:35.552	-22:42:18.896	J2000	1	SN II
V=11.9					
2020yzq	18:22:23.365	+23:28:32.102	J2000	1	SN II
V=11.9					
2020abbl	12:17:52.222	-00:54:28.804	J2000	1	SN II
V=11.9					
2019fya	23:15:16.062	+19:02:29.832	J2000	1	SN II
V=11.9					
SN 2018imf	12:42:41.389	13:15:54.889	J2000	1	SN IIP
V=11.9					
SN 2020scb	00:18:25.624	18:30:59.529	J2000	1	SN Ib/c
V=11.9					
SN 2020fzj	20:15:42.935	-06:18:59.878	J2000	1	SN II
V=11.9					
SN 2018fus	21:02:31.199	-05:37:30.069	J2000	1	SN II
V=11.9					
SN 2020aqb	00:41:37.639	-03:15:12.531	J2000	1	SN IIP
V=11.9					
SN 2019rn	02:17:59.610	14:32:00.399	J2000	1	SN IIb
V=11.9					
SN 2018jq	12:56:48.400	03:53:27.200	J2000	1	SN Ib
V=11.9					
SN 2020abcq	08:44:31.499	-20:20:47.360	J2000	1	SN II
V=11.9					
SN 2019dok	13:46:51.756	16:16:53.731	J2000	1	SN II
V=11.9					

Name	RA	Dec	Coord	Runs	Comment
SN 2019nxk	17:34:05.119	-14:48:31.928	J2000	1	SN II
V=11.9					

Target Notes

This dataset contains 95 galaxies randomly selected from a sample of all galaxies that hosted core-collapse supernovae detected by the ATLAS survey between 2017 and 2021, up to a distance of 100 Mpc, below a declination of 30 degrees, and with no previous MUSE observations. The number of selected galaxies was defined by the time limit of a normal programme (99h), with a total of 1h per target and with some galaxies requiring more than one pointing.

REMARKS & JUSTIFICATIONS

Lunar Phase and Constraints Justification

Please justify here the requested lunar phase and other observing constraints.

Our targets can be observed in any lunar phase as this project is a ‘filler’ program.

Time Justification

Please describe here a detailed computation of the necessary time to execute the observations, including time-critical aspects if any. Parameters used in the ETC should be mentioned so the computation can be reproduced.

Our proposed MUSE observations aim to detect and measure the strength of H II region emission lines throughout target galaxies, together with narrow absorption features in the galaxy continuum. To estimate exposure times, we assume a typical r-band surface brightness of 21 mag per arcsec^2 for faint HII regions (James et al. 2004). We then use the MUSE ETC to estimate our required exposure times. We assume an ‘Infinitely extended source’ and the HII region template (at a redshift of 0.05) together with an r-band surface brightness of 21 mag per arcsec^2. As a ‘filler’ proposal we assume observations to 7 days from new moon with an airmass of 1.4 and seeing 1.5″.

In order to remove the edges of each IFU on the detector (artifacts of the image slicer), it is best to combine observations with all four 90 degree angles. With 4×700 second exposures, the ETC gives a S/N of ~5 in the continuum, which translates to a S/N of more than 100 for all the emission lines we wish to detect (e.g., Hα, [Nii], [O iii], Hβ). This totals roughly 1 hr per pointing.

Most galaxies in our sample are covered by one MUSE pointing, with the exception of 4 targets (SN 2018is, SN 2020hvp, SN 2017ivh, and SN 2020ad) which require more than one MUSE pointings to cover the entire galaxy. We thus require 99 h to observe our sample of 95 host galaxies.

We have previously obtained MUSE data with very similar conditions/observing strategy to that outlined above, and these exposure times allowed us to make the necessary measurements. We have already published several papers based on these data (see publications section). Our team has experts on the reduction, analysis and interpretation of IFS galaxy observations, while IFS data and their analysis can sometimes prove somewhat daunting, our team provides all the required knowledge to fully exploit this rich data set. These data will remain in the archive as a legacy for future extragalactic studies.

Telescope Justification

Please justify why the telescope requested is the best choice for this programme.

MUSE at the VLT is the only currently available IFU instrument that has a FoV of sufficient size to cover the majority of our targets, while at the same time providing high spatial resolution, and sensitivity, allowing targets to be observed in a relatively small amount of time.

We stress here that even in relatively bad seeing conditions we will still be able to unravel kinematic and population substructure in these galaxies over a large FoV. Indeed, even in bad seeing conditions these data will still be better able to probe SN environments and galaxy characteristics than any current or past IFU survey (SAURON, ATLAS3D, CALIFA, SAMI, MaNGA).

Observing Mode Selection

Please explain your choice of SM, VM, or dVM.

Targets are observable throughout the semester, so service mode is required.

Calibration Request

If you need any special calibration not included in the instrument calibration plan, please specify it here.

Standard Calibration.

Duplication with ESO Science Archive

If observations of the same target(s) using the same instrument(s) already exist in the ESO archive, please justify why this programme requests further observations.

We searched for duplications, and there are no IFU observations of these galaxies in the ESO or any other public archive.

GTO Target Duplication Justification

If an instrument GTO team aims at the same target(s), please justify why this programme requests further observations.

n/a

Background and Expertise

Short description of the background, expertise and roles of the various team members in the context of the science case discussed in the proposal. For small teams the applicants may wish to provide a sentence for the qualifications of each member, while for larger teams (e.g. in Large Programmes), only the leading roles need to be specified.

The team has acquired and analysed the vast majority of VLT/MUSE observations of supernova host galaxies. We have tools in place to rapidly leverage the scientific yield of this combined data set. The AMUSING project has run for 11 previous semesters, and has already published >30 papers (for a complete list of publications check https://amusing-muse.github.io/publications/), with many other projects currently ongoing.

T. Pessi is a graduate student working on supernova observations and his thesis is based in using MUSE to study host galaxies of supernovae.
J. Prieto is an expert in supernovae observations and has also worked in host galaxy observations/analysis using MUSE. He is part of the ASAS-SN team.
J. P. Anderson has previously led the AMUSING proposals, and thus has significant experience of data and project organisation. He has expertise in supernova environment studies and how those studies can constrain progenitor scenarios.
J. Lyman is an expert in the study of various transient events and the analysis of SN environments with MUSE. He has developed the code IFUanalysis, which was used to analyze MUSE datacubes of several galaxies that hosted SNe and has been used in several publications of the field
L. Galbany is an expert in studying various supernovae and their host galaxies with integral field spectrograph (IFS) data. He has led and published several works from different campaigns on SNe and their host galaxies, and has expertise in the scheduling, reduction and analysis of VLT data.
S. González-Gaitán is a SN Ia cosmology expert and has led several analyses in large SN surveys (SDSS, SNLS, DES).
H. Kuncarayakti has led MUSE core-collapse SN host galaxies projects (AMUSING, FOSSIL), and is an expert on analysing IFU data.
F. Förster is an expert in supernova observations and astroinformatics, having experience with large transient surveys (HiTS, DES). He is currently leading the ALeRCE project.
S. Srivastav, M. Nicholl, T. Moore, and S. Smartt are experts in the discovery and studies of different transient events, and have lead many important projects in the field. They are part of the ATLAS team.
S. F. Sanchez, F. F. Rosales-Ortega and J. Falcon-Barroso are experts in galaxy formation and evolution, particularly through the use of spectral synthesis with IFS data. They have lead and worked on many projects and publications with data obtained from large IFS galaxy surveys (SDSS, CALIFA, PINGS).
T. Kravtsov is a graduate student working on MUSE observations of SN host galaxies.

REPORT ON PREVIOUS USAGE OF ESO FACILITIES

Run	PI	Instrument	Time	Mode	Comment
111.24UM.001	Thallis Pessi	MUSE	60.0h	Service	Current semester, 78% completed, data to be analyzed.
The local environments of stripped-envelope supernovae					
109.2399.001	Jose Prieto	MUSE	13.0h	Service	Only 3 h were completed so far.
The Extreme Host Galaxy Environments of Low-Luminosity Type Ia SNe with late-time H-alpha emission					
109.2399.002	Jose Prieto	MUSE	4.0h	Service	Only 3 h were completed so far.
The Extreme Host Galaxy Environments of Low-Luminosity Type Ia SNe with late-time H-alpha emission					
0102.D-0095(A)	Joseph Anderson	MUSE	99.0h	Service	Data reduced and analysed. Has contributed to the >30 papers published with AMUSING data thus far.
The All-weather MUse Supernova Integral field Nearby Galaxies (AMUSING) survey VIII: The local environments of type Ia supernovae					
0103.D-0440(B)	Joseph Anderson	MUSE	10.0h	Service	Data reduced and analysed. Has contributed to the >30 papers published with AMUSING data thus far.
The All-weather MUse Supernova Integral field Nearby Galaxies (AMUSING) survey IX: supernova and tidal disruption event rates as a function of environment age and metallicity					
0103.D-0440(A)	Joseph Anderson	MUSE	89.0h	Service	Data reduced and analysed. Has contributed to the >30 papers published with AMUSING data thus far.
The All-weather MUse Supernova Integral field Nearby Galaxies (AMUSING) survey IX: supernova and tidal disruption event rates as a function of environment age and metallicity					
0104.D-0503(A)	Joseph Anderson	MUSE	50.0h	Service	Data reduced and analysed. Has contributed to the >30 papers published with AMUSING data thus far.
The All-weather MUse Supernova Integral field Nearby Galaxies (AMUSING) survey X: star formation in low-mass galaxies as traced by extra-galactic transients					
0104.D-0503(B)	Joseph Anderson	MUSE	49.0h	Service	Data reduced and analysed. Has contributed to the >30 papers published with AMUSING data thus far.
The All-weather MUse Supernova Integral field Nearby Galaxies (AMUSING) survey X: star formation in low-mass galaxies as traced by extra-					

Run	PI	Instrument	Time	Mode	Comment
galactic transients					
0101.D-0748(A)	Hanindyo Kuncarayakti	MUSE	79.0h	Service	Data reduced and analysed. Has contributed to the >30 papers published with AMUSING data thus far.
The All-weather MUse Supernova Integral field Nearby Galaxies (AMUSING) survey VII: Continuing the survey of nebular spectra and environments of core-collapse supernovae					
0101.D-0748(B)	Hanindyo Kuncarayakti	MUSE	20.0h	Service	Data reduced and analysed. Has contributed to the >30 papers published with AMUSING data thus far.
The All-weather MUse Supernova Integral field Nearby Galaxies (AMUSING) survey VII: Continuing the survey of nebular spectra and environments of core-collapse supernovae					
111.24VQ.001	Timo Kravtsov	MUSE	54.0h	Service	Current semester.
Environment constraints on supernovae Ibn: high or low mass progenitors?					

RECENT PI/CoIs PUBLICATIONS MOST RELEVANT TO THE SUBJECT OF THIS PROPOSAL

1. Pessi, T., et al. (2023) "A characterization of ASAS-SN core-collapse supernova environments with VLT+MUSE. I. Sample selection, analysis of local environments, and correlations with light curve properties," A&A, 677, A28 - 2023A&A...677A..28P
2. Pessi, T., Anderson, J. P., Lyman, J. D., et al. (2023) "A metallicity dependence on the occurrence of core-collapse supernovae," arXiv, arXiv:2306.11962 - 2023arXiv230611962P
3. López-Cobá, C., Sánchez, S. F., Lin, L., et al. (2022) "Exploring Stellar and Ionized Gas Noncircular Motions in Barred Galaxies with MUSE," ApJ, 939, 40 - 2022ApJ...939...40L
4. Nicholl, M., Srivastav, S., Fulton, M. D., et al. (2023) "AT 2022aedm and a New Class of Luminous, Fast-cooling Transients in Elliptical Galaxies," ApJL, 954, L28 - 2023ApJ...954L..28N
5. Moriya, T. J., Galbany, L., Jiménez-Palau, C., et al. (2023) "Environmental dependence of Type IIn supernova properties," A&A, 677, A20 - 2023A&A...677A..20M
6. Cleland, C., McGee, S. L., & Nicholl, M. (2023) "Metallicity beats sSFR: the connection between superluminous supernova host galaxy environments and the importance of metallicity for their production," MNRAS, 524, 3559-3567 - 2023MNRAS.524.3559C
7. Srivastav, S., Smartt, S. J., Huber, M. E., et al. (2022) "SN 2020kyg and the rates of faint Iax supernovae from ATLAS," MNRAS, 511, 2708-2731 - 2022MNRAS.511.2708S
8. Robleto-Orús, A. C., Torres-Papaqui, J. P., Longinotti, A. L., et al. (2021) "A MUSE study of NGC 7469: Spatially resolved star-formation and AGN-driven outflows," IAUS, 359, 291-294 - 2021IAUS..359..291R
9. Srivastav, S., Moore, T., Nicholl, M., et al. (2023) "Unprecedented early flux excess in the hybrid 02es-like type Ia supernova 2022ywc indicates interaction with circumstellar material," arXiv, arXiv:2308.06019 - 2023arXiv230806019S
10. Grayling, M., Gutiérrez, C. P., Sullivan, M., et al. (2023) "Core-collapse supernovae in the Dark Energy Survey: luminosity functions and host galaxy demographics," MNRAS, 520, 684-701 - 2023MNRAS.520..684G
11. Uddin, S. A., Burns, C. R., Phillips, M. M., et al. (2023) "Carnegie Supernova Project-I and -II: Measurements of H_0 using Cepheid, TRGB, and SBF Distance Calibration to Type Ia Supernovae," arXiv, arXiv:2308.01875 - 2023arXiv230801875U

INVESTIGATORS

Thallis Pessi, Universidad Diego Portales, Chile (PI)
Jose Prieto, Universidad Diego Portales, Chile
Joseph Anderson, ESO Chile, ESO
Joseph Lyman, University of Warwick, United Kingdom
Shubham Srivastav, Queen's University - Belfast, United Kingdom
Matt Nicholl, Queen's University - Belfast, United Kingdom
Thomas Moore, Queen's University - Belfast, United Kingdom
Stephen Smartt, University of Oxford, United Kingdom
Lluis Galbany, Institut d'Estudis Espacials de Catalunya - Barcelona, Spain
Jesus Falcon-Barroso, Instituto de Astrofisica de Canarias, Spain
Santiago Gonzalez Gaitan, Universidade de Lisboa, Portugal
Hanindyo Kuncarayakti, Turun yliopisto, Finland
Francisco Forster, Universidad de Chile, Chile
Fernando Fabian Rosales-Ortega, Instituto Nacional de Astrofísica, Óptica y Electrónica, Mexico

Timo Kravtsov, ESO Chile, ESO

OBSERVATIONS

In the table below, the repeat factor is applied to the complete observation on that target, including its overhead.

✔ The PI acknowledged that all the telescope times listed below include overheads.

Run 113.26FT.001 • Run 1 • P113 • MUSE • SM — Tel. Time: 99h00m

FLI: 100% • Turb.: 85% • pwv: 30.0mm • Sky: Variable, thin cirrus • Airmass: 2.8

Target • 2020ocz • 05:10:44.202 • -31:35:37.522 — Tel. Time: 01h00m

OS 1	WFM-NOAO	Observation
Tel. Time: 900 s	Instrument Mode: WFM-NOAO-N	Integration Time: 0 s
Repeat: 4 x	Telescope Overheads: 360 s	Instrument Overheads: 0 s
Total Tel. Time: 3600s		Signal/Noise: 0.0

Target • 2019ejj • 08:07:08.776 • -28:03:11.642 — Tel. Time: 01h00m

OS 1	WFM-NOAO	Observation
Tel. Time: 900 s	Instrument Mode: WFM-NOAO-N	Integration Time: 0 s
Repeat: 4 x	Telescope Overheads: 360 s	Instrument Overheads: 0 s
Total Tel. Time: 3600s		Signal/Noise: 0.0

Target • 2018ke • 13:08:39.531 • -41:27:16.366 — Tel. Time: 01h00m

OS 1	WFM-NOAO	Observation
Tel. Time: 900 s	Instrument Mode: WFM-NOAO-N	Integration Time: 0 s
Repeat: 4 x	Telescope Overheads: 360 s	Instrument Overheads: 0 s
Total Tel. Time: 3600s		Signal/Noise: 0.0

Target • 2018ecf • 14:06:34.388 • -34:18:04.079 — Tel. Time: 01h00m

OS 1	WFM-NOAO	Observation
Tel. Time: 900 s	Instrument Mode: WFM-NOAO-N	Integration Time: 0 s
Repeat: 4 x	Telescope Overheads: 360 s	Instrument Overheads: 0 s
Total Tel. Time: 3600s		Signal/Noise: 0.0

Target • 2017izl • 13:19:55.343 • -47:17:05.489 — Tel. Time: 01h00m

OS 1	WFM-NOAO	Observation
Tel. Time: 900 s	Instrument Mode: WFM-NOAO-N	Integration Time: 0 s
Repeat: 4 x	Telescope Overheads: 360 s	Instrument Overheads: 0 s
Total Tel. Time: 3600s		Signal/Noise: 0.0

Target • 2020ad • 13:57:56.805 • -29:17:07.379 — Tel. Time: 03h00m

OS 1	WFM-NOAO	Observation
Tel. Time: 900 s	Instrument Mode: WFM-NOAO-N	Integration Time: 0 s
Repeat: 12 x	Telescope Overheads: 360 s	Instrument Overheads: 0 s
Total Tel. Time: 03h00m		Signal/Noise: 0.0

Target • 2020bfb • 12:54:44.220 • -39:51:09.536 — Tel. Time: 01h00m

OS 1	WFM-NOAO	Observation
Tel. Time: 900 s	Instrument Mode: WFM-NOAO-N	Integration Time: 0 s
Repeat: 4 x	Telescope Overheads: 360 s	Instrument Overheads: 0 s
Total Tel. Time: 3600s		Signal/Noise: 0.0

Target • 2020admc • 11:54:06.067 • -39:51:52.715 — Tel. Time: 01h00m

OS 1	WFM-NOAO	Observation
Tel. Time: 900 s	Instrument Mode: WFM-NOAO-N	Integration Time: 0 s
Repeat: 4 x	Telescope Overheads: 360 s	Instrument Overheads: 0 s
Total Tel. Time: 3600s		Signal/Noise: 0.0

Target • 2020acpi • 11:35:46.563 • -49:02:12.257 — Tel. Time: 01h00m

OS 1	WFM-NOAO	Observation
Tel. Time: 900 s	Instrument Mode: WFM-NOAO-N	Integration Time: 0 s
Repeat: 4 x	Telescope Overheads: 360 s	Instrument Overheads: 0 s
Total Tel. Time: 3600s		Signal/Noise: 0.0

Target • 2021bmw • 13:47:39.716 • -29:25:54.620 — Tel. Time: 01h00m

OS 1	WFM-NOAO	Observation
Tel. Time: 900 s	Instrument Mode: WFM-NOAO-N	Integration Time: 0 s
Repeat: 4 x	Telescope Overheads: 360 s	Instrument Overheads: 0 s
Total Tel. Time: 3600s		Signal/Noise: 0.0

Target • 2018ass • 21:10:19.010 • -29:31:22.253 Tel. Time: 01h00m

OS 1	WFM-NOAO	Observation
Tel. Time: 900 s	Instrument Mode: WFM-NOAO-N	Integration Time: 0 s
Repeat: 4 x	Telescope Overheads: 360 s	Instrument Overheads: 0 s
Total Tel. Time: 3600s		Signal/Noise: 0.0

Target • 2019cwt • 20:00:40.210 • -34:47:43.040 Tel. Time: 01h00m

OS 1	WFM-NOAO	Observation
Tel. Time: 900 s	Instrument Mode: WFM-NOAO-N	Integration Time: 0 s
Repeat: 4 x	Telescope Overheads: 360 s	Instrument Overheads: 0 s
Total Tel. Time: 3600s		Signal/Noise: 0.0

Target • 2018cmj • 01:38:53.322 • -42:35:22.394 Tel. Time: 01h00m

OS 1	WFM-NOAO	Observation
Tel. Time: 900 s	Instrument Mode: WFM-NOAO-N	Integration Time: 0 s
Repeat: 4 x	Telescope Overheads: 360 s	Instrument Overheads: 0 s
Total Tel. Time: 3600s		Signal/Noise: 0.0

Target • 2020zae • 20:07:47.943 • -29:48:49.982 Tel. Time: 01h00m

OS 1	WFM-NOAO	Observation
Tel. Time: 900 s	Instrument Mode: WFM-NOAO-N	Integration Time: 0 s
Repeat: 4 x	Telescope Overheads: 360 s	Instrument Overheads: 0 s
Total Tel. Time: 3600s		Signal/Noise: 0.0

Target • 2019gvp • 16:46:35.511 • -31:35:30.894 Tel. Time: 01h00m

OS 1	WFM-NOAO	Observation
Tel. Time: 900 s	Instrument Mode: WFM-NOAO-N	Integration Time: 0 s
Repeat: 4 x	Telescope Overheads: 360 s	Instrument Overheads: 0 s
Total Tel. Time: 3600s		Signal/Noise: 0.0

Target • 2020mrj • 14:24:24.462 • -28:37:54.430 Tel. Time: 01h00m

OS 1	WFM-NOAO	Observation
Tel. Time: 900 s	Instrument Mode: WFM-NOAO-N	Integration Time: 0 s
Repeat: 4 x	Telescope Overheads: 360 s	Instrument Overheads: 0 s
Total Tel. Time: 3600s		Signal/Noise: 0.0

Target • 2020voh • 23:03:40.285 • -36:01:40.354 Tel. Time: 01h00m

OS 1	WFM-NOAO	Observation
Tel. Time: 900 s	Instrument Mode: WFM-NOAO-N	Integration Time: 0 s
Repeat: 4 x	Telescope Overheads: 360 s	Instrument Overheads: 0 s
Total Tel. Time: 3600s		Signal/Noise: 0.0

Target • 2020mvk • 13:35:45.684 • -30:52:30.396 Tel. Time: 01h00m

OS 1	WFM-NOAO	Observation
Tel. Time: 900 s	Instrument Mode: WFM-NOAO-N	Integration Time: 0 s
Repeat: 4 x	Telescope Overheads: 360 s	Instrument Overheads: 0 s
Total Tel. Time: 3600s		Signal/Noise: 0.0

Target • 2021aez • 15:36:03.959 • -37:18:04.306 Tel. Time: 01h00m

OS 1	WFM-NOAO	Observation
Tel. Time: 900 s	Instrument Mode: WFM-NOAO-N	Integration Time: 0 s
Repeat: 4 x	Telescope Overheads: 360 s	Instrument Overheads: 0 s
Total Tel. Time: 3600s		Signal/Noise: 0.0

Target • 2020aboq • 06:38:23.738 • -35:13:29.114 Tel. Time: 01h00m

OS 1	WFM-NOAO	Observation
Tel. Time: 900 s	Instrument Mode: WFM-NOAO-N	Integration Time: 0 s
Repeat: 4 x	Telescope Overheads: 360 s	Instrument Overheads: 0 s
Total Tel. Time: 3600s		Signal/Noise: 0.0

Target • 2017hhx • 22:00:32.920 • -27:13:29.478 — Tel. Time: 01h00m

OS 1	WFM-NOAO	Observation
Tel. Time: 900 s	Instrument Mode: WFM-NOAO-N	Integration Time: 0 s
Repeat: 4 x	Telescope Overheads: 360 s	Instrument Overheads: 0 s
Total Tel. Time: 3600s		Signal/Noise: 0.0

Target • 2017hxj • 23:58:00.701 • -41:32:02.706 — Tel. Time: 01h00m

OS 1	WFM-NOAO	Observation
Tel. Time: 900 s	Instrument Mode: WFM-NOAO-N	Integration Time: 0 s
Repeat: 4 x	Telescope Overheads: 360 s	Instrument Overheads: 0 s
Total Tel. Time: 3600s		Signal/Noise: 0.0

Target • 2018dza • 14:49:17.991 • -30:17:22.297 — Tel. Time: 01h00m

OS 1	WFM-NOAO	Observation
Tel. Time: 900 s	Instrument Mode: WFM-NOAO-N	Integration Time: 0 s
Repeat: 4 x	Telescope Overheads: 360 s	Instrument Overheads: 0 s
Total Tel. Time: 3600s		Signal/Noise: 0.0

Target • 2018emt • 22:10:35.660 • -27:14:58.697 — Tel. Time: 01h00m

OS 1	WFM-NOAO	Observation
Tel. Time: 900 s	Instrument Mode: WFM-NOAO-N	Integration Time: 0 s
Repeat: 4 x	Telescope Overheads: 360 s	Instrument Overheads: 0 s
Total Tel. Time: 3600s		Signal/Noise: 0.0

Target • 2019thi • 11:15:15.322 • -27:39:11.822 — Tel. Time: 01h00m

OS 1	WFM-NOAO	Observation
Tel. Time: 900 s	Instrument Mode: WFM-NOAO-N	Integration Time: 0 s
Repeat: 4 x	Telescope Overheads: 360 s	Instrument Overheads: 0 s
Total Tel. Time: 3600s		Signal/Noise: 0.0

Target • 2019xtw • 02:43:33.630 • -38:37:30.720 — Tel. Time: 01h00m

OS 1	WFM-NOAO	Observation
Tel. Time: 900 s	Instrument Mode: WFM-NOAO-N	Integration Time: 0 s
Repeat: 4 x	Telescope Overheads: 360 s	Instrument Overheads: 0 s
Total Tel. Time: 3600s		Signal/Noise: 0.0

Target • 2019axz • 14:30:16.676 • -43:33:41.094 — Tel. Time: 01h00m

OS 1	WFM-NOAO	Observation
Tel. Time: 900 s	Instrument Mode: WFM-NOAO-N	Integration Time: 0 s
Repeat: 4 x	Telescope Overheads: 360 s	Instrument Overheads: 0 s
Total Tel. Time: 3600s		Signal/Noise: 0.0

Target • 2019nyn • 01:07:37.207 • -41:51:12.348 — Tel. Time: 01h00m

OS 1	WFM-NOAO	Observation
Tel. Time: 900 s	Instrument Mode: WFM-NOAO-N	Integration Time: 0 s
Repeat: 4 x	Telescope Overheads: 360 s	Instrument Overheads: 0 s
Total Tel. Time: 3600s		Signal/Noise: 0.0

Target • 2019ofc • 01:33:36.919 • -38:35:59.014 — Tel. Time: 01h00m

OS 1	WFM-NOAO	Observation
Tel. Time: 900 s	Instrument Mode: WFM-NOAO-N	Integration Time: 0 s
Repeat: 4 x	Telescope Overheads: 360 s	Instrument Overheads: 0 s
Total Tel. Time: 3600s		Signal/Noise: 0.0

Target • 2019uhm • 10:28:48.470 • -31:29:52.076 — Tel. Time: 01h00m

OS 1	WFM-NOAO	Observation
Tel. Time: 900 s	Instrument Mode: WFM-NOAO-N	Integration Time: 0 s
Repeat: 4 x	Telescope Overheads: 360 s	Instrument Overheads: 0 s
Total Tel. Time: 3600s		Signal/Noise: 0.0

Target • 2020cnu • 04:24:08.165 • -27:04:47.593 — Tel. Time: 01h00m

OS 1	WFM-NOAO	Observation
Tel. Time: 900 s	Instrument Mode: WFM-NOAO-N	Integration Time: 0 s
Repeat: 4 x	Telescope Overheads: 360 s	Instrument Overheads: 0 s

Total Tel. Time: 3600s		Signal/Noise: 0.0

Target • 2019dna • 21:05:23.801 • +19:44:34.375 Tel. Time: 01h00m

OS 1	WFM-NOAO	Observation
Tel. Time: 900 s	Instrument Mode: WFM-NOAO-N	Integration Time: 0 s
Repeat: 4 x	Telescope Overheads: 360 s	Instrument Overheads: 0 s
Total Tel. Time: 3600s		Signal/Noise: 0.0

Target • 2017ixz • 07:47:03.056 • +26:46:25.936 Tel. Time: 01h00m

OS 1	WFM-NOAO	Observation
Tel. Time: 900 s	Instrument Mode: WFM-NOAO-N	Integration Time: 0 s
Repeat: 4 x	Telescope Overheads: 360 s	Instrument Overheads: 0 s
Total Tel. Time: 3600s		Signal/Noise: 0.0

Target • 2020obd • 02:28:35.910 • -10:32:18.758 Tel. Time: 01h00m

OS 1	WFM-NOAO	Observation
Tel. Time: 900 s	Instrument Mode: WFM-NOAO-N	Integration Time: 0 s
Repeat: 4 x	Telescope Overheads: 360 s	Instrument Overheads: 0 s
Total Tel. Time: 3600s		Signal/Noise: 0.0

Target • 2018fy • 09:53:20.020 • -18:25:09.786 Tel. Time: 01h00m

OS 1	WFM-NOAO	Observation
Tel. Time: 900 s	Instrument Mode: WFM-NOAO-N	Integration Time: 0 s
Repeat: 4 x	Telescope Overheads: 360 s	Instrument Overheads: 0 s
Total Tel. Time: 3600s		Signal/Noise: 0.0

Target • 2017ivh • 13:39:36.252 • -11:28:55.884 Tel. Time: 02h00m

OS 1	WFM-NOAO	Observation
Tel. Time: 900 s	Instrument Mode: WFM-NOAO-N	Integration Time: 0 s
Repeat: 8 x	Telescope Overheads: 360 s	Instrument Overheads: 0 s
Total Tel. Time: 7200s		Signal/Noise: 0.0

Target • 2019pad • 15:03:44.238 • -03:17:47.080 Tel. Time: 01h00m

OS 1	WFM-NOAO	Observation
Tel. Time: 900 s	Instrument Mode: WFM-NOAO-N	Integration Time: 0 s
Repeat: 4 x	Telescope Overheads: 360 s	Instrument Overheads: 0 s
Total Tel. Time: 3600s		Signal/Noise: 0.0

Target • 2019ovq • 04:10:18.717 • +13:24:14.875 Tel. Time: 01h00m

OS 1	WFM-NOAO	Observation
Tel. Time: 900 s	Instrument Mode: WFM-NOAO-N	Integration Time: 0 s
Repeat: 4 x	Telescope Overheads: 360 s	Instrument Overheads: 0 s
Total Tel. Time: 3600s		Signal/Noise: 0.0

Target • 2018is • 13:16:57.347 • -16:37:04.181 Tel. Time: 02h00m

OS 1	WFM-NOAO	Observation
Tel. Time: 900 s	Instrument Mode: WFM-NOAO-N	Integration Time: 0 s
Repeat: 8 x	Telescope Overheads: 360 s	Instrument Overheads: 0 s
Total Tel. Time: 7200s		Signal/Noise: 0.0

Target • 2018imj • 06:51:05.759 • +12:54:55.642 Tel. Time: 01h00m

OS 1	WFM-NOAO	Observation
Tel. Time: 900 s	Instrument Mode: WFM-NOAO-N	Integration Time: 0 s
Repeat: 4 x	Telescope Overheads: 360 s	Instrument Overheads: 0 s
Total Tel. Time: 3600s		Signal/Noise: 0.0

Target • 2020fsb • 15:39:03.810 • -25:58:28.240 Tel. Time: 01h00m

OS 1	WFM-NOAO	Observation
Tel. Time: 900 s	Instrument Mode: WFM-NOAO-N	Integration Time: 0 s
Repeat: 4 x	Telescope Overheads: 360 s	Instrument Overheads: 0 s
Total Tel. Time: 3600s		Signal/Noise: 0.0

Target • 2020abjq • 01:06:14.630 • +03:34:26.112 Tel. Time: 01h00m

OS 1	WFM-NOAO	Observation
Tel. Time: 900 s	Instrument Mode: WFM-NOAO-N	Integration Time: 0 s

Repeat: 4 x	Telescope Overheads: 360 s	Instrument Overheads: 0 s
Total Tel. Time: 3600s		Signal/Noise: 0.0

Target • 2020qbu • 01:33:53.394 • -13:04:49.184 Tel. Time: 01h00m

OS 1	WFM-NOAO	Observation
Tel. Time: 900 s	Instrument Mode: WFM-NOAO-N	Integration Time: 0 s
Repeat: 4 x	Telescope Overheads: 360 s	Instrument Overheads: 0 s
Total Tel. Time: 3600s		Signal/Noise: 0.0

Target • 2019edo • 12:11:51.587 • +24:08:11.753 Tel. Time: 01h00m

OS 1	WFM-NOAO	Observation
Tel. Time: 900 s	Instrument Mode: WFM-NOAO-N	Integration Time: 0 s
Repeat: 4 x	Telescope Overheads: 360 s	Instrument Overheads: 0 s
Total Tel. Time: 3600s		Signal/Noise: 0.0

Target • 2017hqj • 21:05:39.017 • +11:24:31.784 Tel. Time: 01h00m

OS 1	WFM-NOAO	Observation
Tel. Time: 900 s	Instrument Mode: WFM-NOAO-N	Integration Time: 0 s
Repeat: 4 x	Telescope Overheads: 360 s	Instrument Overheads: 0 s
Total Tel. Time: 3600s		Signal/Noise: 0.0

Target • 2021duv • 11:45:54.636 • +22:27:16.448 Tel. Time: 01h00m

OS 1	WFM-NOAO	Observation
Tel. Time: 900 s	Instrument Mode: WFM-NOAO-N	Integration Time: 0 s
Repeat: 4 x	Telescope Overheads: 360 s	Instrument Overheads: 0 s
Total Tel. Time: 3600s		Signal/Noise: 0.0

Target • 2018hhr • 02:55:48.931 • +01:04:42.528 Tel. Time: 01h00m

OS 1	WFM-NOAO	Observation
Tel. Time: 900 s	Instrument Mode: WFM-NOAO-N	Integration Time: 0 s
Repeat: 4 x	Telescope Overheads: 360 s	Instrument Overheads: 0 s
Total Tel. Time: 3600s		Signal/Noise: 0.0

Target • 2020mjm • 14:29:29.331 • -00:01:17.767 Tel. Time: 01h00m

OS 1	WFM-NOAO	Observation
Tel. Time: 900 s	Instrument Mode: WFM-NOAO-N	Integration Time: 0 s
Repeat: 4 x	Telescope Overheads: 360 s	Instrument Overheads: 0 s
Total Tel. Time: 3600s		Signal/Noise: 0.0

Target • 2020nja • 01:34:34.688 • -03:20:37.669 Tel. Time: 01h00m

OS 1	WFM-NOAO	Observation
Tel. Time: 900 s	Instrument Mode: WFM-NOAO-N	Integration Time: 0 s
Repeat: 4 x	Telescope Overheads: 360 s	Instrument Overheads: 0 s
Total Tel. Time: 3600s		Signal/Noise: 0.0

Target • 2018hjx • 03:24:55.582 • -02:49:19.736 Tel. Time: 01h00m

OS 1	WFM-NOAO	Observation
Tel. Time: 900 s	Instrument Mode: WFM-NOAO-N	Integration Time: 0 s
Repeat: 4 x	Telescope Overheads: 360 s	Instrument Overheads: 0 s
Total Tel. Time: 3600s		Signal/Noise: 0.0

Target • 2020twk • 23:29:13.482 • -02:05:42.018 Tel. Time: 01h00m

OS 1	WFM-NOAO	Observation
Tel. Time: 900 s	Instrument Mode: WFM-NOAO-N	Integration Time: 0 s
Repeat: 4 x	Telescope Overheads: 360 s	Instrument Overheads: 0 s
Total Tel. Time: 3600s		Signal/Noise: 0.0

Target • 2020njz • 02:01:51.016 • -10:28:11.827 Tel. Time: 01h00m

OS 1	WFM-NOAO	Observation
Tel. Time: 900 s	Instrument Mode: WFM-NOAO-N	Integration Time: 0 s
Repeat: 4 x	Telescope Overheads: 360 s	Instrument Overheads: 0 s
Total Tel. Time: 3600s		Signal/Noise: 0.0

Target • 2019leu • 19:05:16.366 • +27:00:25.531 Tel. Time: 01h00m

OS 1	WFM-NOAO	Observation

Tel. Time: 900 s Repeat: 4 x Total Tel. Time: 3600s	Instrument Mode: WFM-NOAO-N Telescope Overheads: 360 s	Integration Time: 0 s Instrument Overheads: 0 s Signal/Noise: 0.0

Target • 2018ino • 11:26:42.522 • +20:43:37.052 Tel. Time: 01h00m

OS 1	WFM-NOAO	Observation
Tel. Time: 900 s Repeat: 4 x Total Tel. Time: 3600s	Instrument Mode: WFM-NOAO-N Telescope Overheads: 360 s	Integration Time: 0 s Instrument Overheads: 0 s Signal/Noise: 0.0

Target • 2019jyw • 01:06:30.211 • -02:11:56.303 Tel. Time: 01h00m

OS 1	WFM-NOAO	Observation
Tel. Time: 900 s Repeat: 4 x Total Tel. Time: 3600s	Instrument Mode: WFM-NOAO-N Telescope Overheads: 360 s	Integration Time: 0 s Instrument Overheads: 0 s Signal/Noise: 0.0

Target • 2020igs • 09:36:55.416 • +08:33:44.554 Tel. Time: 01h00m

OS 1	WFM-NOAO	Observation
Tel. Time: 900 s Repeat: 4 x Total Tel. Time: 3600s	Instrument Mode: WFM-NOAO-N Telescope Overheads: 360 s	Integration Time: 0 s Instrument Overheads: 0 s Signal/Noise: 0.0

Target • 2019abb • 07:54:17.275 • +14:16:23.257 Tel. Time: 01h00m

OS 1	WFM-NOAO	Observation
Tel. Time: 900 s Repeat: 4 x Total Tel. Time: 3600s	Instrument Mode: WFM-NOAO-N Telescope Overheads: 360 s	Integration Time: 0 s Instrument Overheads: 0 s Signal/Noise: 0.0

Target • 2017hpn • 09:08:01.713 • +27:15:04.720 Tel. Time: 01h00m

OS 1	WFM-NOAO	Observation
Tel. Time: 900 s Repeat: 4 x Total Tel. Time: 3600s	Instrument Mode: WFM-NOAO-N Telescope Overheads: 360 s	Integration Time: 0 s Instrument Overheads: 0 s Signal/Noise: 0.0

Target • 2018dht • 20:55:19.057 • +00:32:18.784 Tel. Time: 01h00m

OS 1	WFM-NOAO	Observation
Tel. Time: 900 s Repeat: 4 x Total Tel. Time: 3600s	Instrument Mode: WFM-NOAO-N Telescope Overheads: 360 s	Integration Time: 0 s Instrument Overheads: 0 s Signal/Noise: 0.0

Target • 2018hij • 08:24:30.551 • +18:36:15.286 Tel. Time: 01h00m

OS 1	WFM-NOAO	Observation
Tel. Time: 900 s Repeat: 4 x Total Tel. Time: 3600s	Instrument Mode: WFM-NOAO-N Telescope Overheads: 360 s	Integration Time: 0 s Instrument Overheads: 0 s Signal/Noise: 0.0

Target • 2017hyh • 07:10:41.078 • +06:27:41.281 Tel. Time: 01h00m

OS 1	WFM-NOAO	Observation
Tel. Time: 900 s Repeat: 4 x Total Tel. Time: 3600s	Instrument Mode: WFM-NOAO-N Telescope Overheads: 360 s	Integration Time: 0 s Instrument Overheads: 0 s Signal/Noise: 0.0

Target • 2019yc • 00:39:34.990 • +00:52:04.310 Tel. Time: 01h00m

OS 1	WFM-NOAO	Observation
Tel. Time: 900 s Repeat: 4 x Total Tel. Time: 3600s	Instrument Mode: WFM-NOAO-N Telescope Overheads: 360 s	Integration Time: 0 s Instrument Overheads: 0 s Signal/Noise: 0.0

Target • 2019gqm • 19:48:09.566 • -24:26:36.337 Tel. Time: 01h00m

OS 1	WFM-NOAO	Observation
Tel. Time: 900 s Repeat: 4 x Total Tel. Time: 3600s	Instrument Mode: WFM-NOAO-N Telescope Overheads: 360 s	Integration Time: 0 s Instrument Overheads: 0 s Signal/Noise: 0.0

Target • 2018cup • 12:35:22.969 • +29:29:31.888 Tel. Time: 01h00m

OS 1	WFM-NOAO	Observation
Tel. Time: 900 s	Instrument Mode: WFM-NOAO-N	Integration Time: 0 s
Repeat: 4 x	Telescope Overheads: 360 s	Instrument Overheads: 0 s
Total Tel. Time: 3600s		Signal/Noise: 0.0

Target • 2019hqm • 17:36:56.190 • +21:06:17.600 Tel. Time: 01h00m

OS 1	WFM-NOAO	Observation
Tel. Time: 900 s	Instrument Mode: WFM-NOAO-N	Integration Time: 0 s
Repeat: 4 x	Telescope Overheads: 360 s	Instrument Overheads: 0 s
Total Tel. Time: 3600s		Signal/Noise: 0.0

Target • 2020hop • 13:19:28.193 • -13:43:25.241 Tel. Time: 01h00m

OS 1	WFM-NOAO	Observation
Tel. Time: 900 s	Instrument Mode: WFM-NOAO-N	Integration Time: 0 s
Repeat: 4 x	Telescope Overheads: 360 s	Instrument Overheads: 0 s
Total Tel. Time: 3600s		Signal/Noise: 0.0

Target • 2020zgl • 23:28:01.148 • -02:09:53.636 Tel. Time: 01h00m

OS 1	WFM-NOAO	Observation
Tel. Time: 900 s	Instrument Mode: WFM-NOAO-N	Integration Time: 0 s
Repeat: 4 x	Telescope Overheads: 360 s	Instrument Overheads: 0 s
Total Tel. Time: 3600s		Signal/Noise: 0.0

Target • 2017iit • 05:03:20.154 • +18:27:03.031 Tel. Time: 01h00m

OS 1	WFM-NOAO	Observation
Tel. Time: 900 s	Instrument Mode: WFM-NOAO-N	Integration Time: 0 s
Repeat: 4 x	Telescope Overheads: 360 s	Instrument Overheads: 0 s
Total Tel. Time: 3600s		Signal/Noise: 0.0

Target • 2019sox • 21:31:24.722 • +02:29:39.016 Tel. Time: 01h00m

OS 1	WFM-NOAO	Observation
Tel. Time: 900 s	Instrument Mode: WFM-NOAO-N	Integration Time: 0 s
Repeat: 4 x	Telescope Overheads: 360 s	Instrument Overheads: 0 s
Total Tel. Time: 3600s		Signal/Noise: 0.0

Target • 2020aqy • 15:01:54.667 • +25:57:59.051 Tel. Time: 01h00m

OS 1	WFM-NOAO	Observation
Tel. Time: 900 s	Instrument Mode: WFM-NOAO-N	Integration Time: 0 s
Repeat: 4 x	Telescope Overheads: 360 s	Instrument Overheads: 0 s
Total Tel. Time: 3600s		Signal/Noise: 0.0

Target • 2019bkc • 10:00:22.548 • -03:01:12.558 Tel. Time: 01h00m

OS 1	WFM-NOAO	Observation
Tel. Time: 900 s	Instrument Mode: WFM-NOAO-N	Integration Time: 0 s
Repeat: 4 x	Telescope Overheads: 360 s	Instrument Overheads: 0 s
Total Tel. Time: 3600s		Signal/Noise: 0.0

Target • 2020ovk • 23:54:17.730 • +26:19:36.131 Tel. Time: 01h00m

OS 1	WFM-NOAO	Observation
Tel. Time: 900 s	Instrument Mode: WFM-NOAO-N	Integration Time: 0 s
Repeat: 4 x	Telescope Overheads: 360 s	Instrument Overheads: 0 s
Total Tel. Time: 3600s		Signal/Noise: 0.0

Target • 2019tsf • 11:08:32.790 • -10:28:54.365 Tel. Time: 01h00m

OS 1	WFM-NOAO	Observation
Tel. Time: 900 s	Instrument Mode: WFM-NOAO-N	Integration Time: 0 s
Repeat: 4 x	Telescope Overheads: 360 s	Instrument Overheads: 0 s
Total Tel. Time: 3600s		Signal/Noise: 0.0

Target • 2020hvp • 16:21:45.394 • -02:17:21.322 Tel. Time: 02h00m

OS 1	WFM-NOAO	Observation
Tel. Time: 900 s	Instrument Mode: WFM-NOAO-N	Integration Time: 0 s
Repeat: 8 x	Telescope Overheads: 360 s	Instrument Overheads: 0 s
Total Tel. Time: 7200s		Signal/Noise: 0.0

Target • 2018fer • 20:33:05.235 • -20:51:24.390 Tel. Time: 01h00m

OS 1	WFM-NOAO	Observation
Tel. Time: 900 s	Instrument Mode: WFM-NOAO-N	Integration Time: 0 s
Repeat: 4 x	Telescope Overheads: 360 s	Instrument Overheads: 0 s
Total Tel. Time: 3600s		Signal/Noise: 0.0

Target • 2019dtt • 22:34:37.507 • +00:10:32.628 Tel. Time: 01h00m

OS 1	WFM-NOAO	Observation
Tel. Time: 900 s	Instrument Mode: WFM-NOAO-N	Integration Time: 0 s
Repeat: 4 x	Telescope Overheads: 360 s	Instrument Overheads: 0 s
Total Tel. Time: 3600s		Signal/Noise: 0.0

Target • 2019aax • 12:17:05.658 • -26:37:44.620 Tel. Time: 01h00m

OS 1	WFM-NOAO	Observation
Tel. Time: 900 s	Instrument Mode: WFM-NOAO-N	Integration Time: 0 s
Repeat: 4 x	Telescope Overheads: 360 s	Instrument Overheads: 0 s
Total Tel. Time: 3600s		Signal/Noise: 0.0

Target • 2018bvi • 14:14:18.412 • +10:40:41.722 Tel. Time: 01h00m

OS 1	WFM-NOAO	Observation
Tel. Time: 900 s	Instrument Mode: WFM-NOAO-N	Integration Time: 0 s
Repeat: 4 x	Telescope Overheads: 360 s	Instrument Overheads: 0 s
Total Tel. Time: 3600s		Signal/Noise: 0.0

Target • 2018ub • 11:54:58.712 • +06:19:47.294 Tel. Time: 01h00m

OS 1	WFM-NOAO	Observation
Tel. Time: 900 s	Instrument Mode: WFM-NOAO-N	Integration Time: 0 s
Repeat: 4 x	Telescope Overheads: 360 s	Instrument Overheads: 0 s
Total Tel. Time: 3600s		Signal/Noise: 0.0

Target • 2018fcx • 04:05:56.717 • -15:08:43.595 Tel. Time: 01h00m

OS 1	WFM-NOAO	Observation
Tel. Time: 900 s	Instrument Mode: WFM-NOAO-N	Integration Time: 0 s
Repeat: 4 x	Telescope Overheads: 360 s	Instrument Overheads: 0 s
Total Tel. Time: 3600s		Signal/Noise: 0.0

Target • 2020pub • 10:37:35.552 • -22:42:18.896 Tel. Time: 01h00m

OS 1	WFM-NOAO	Observation
Tel. Time: 900 s	Instrument Mode: WFM-NOAO-N	Integration Time: 0 s
Repeat: 4 x	Telescope Overheads: 360 s	Instrument Overheads: 0 s
Total Tel. Time: 3600s		Signal/Noise: 0.0

Target • 2020yzq • 18:22:23.365 • +23:28:32.102 Tel. Time: 01h00m

OS 1	WFM-NOAO	Observation
Tel. Time: 900 s	Instrument Mode: WFM-NOAO-N	Integration Time: 0 s
Repeat: 4 x	Telescope Overheads: 360 s	Instrument Overheads: 0 s
Total Tel. Time: 3600s		Signal/Noise: 0.0

Target • 2020abbl • 12:17:52.222 • -00:54:28.804 Tel. Time: 01h00m

OS 1	WFM-NOAO	Observation
Tel. Time: 900 s	Instrument Mode: WFM-NOAO-N	Integration Time: 0 s
Repeat: 4 x	Telescope Overheads: 360 s	Instrument Overheads: 0 s
Total Tel. Time: 3600s		Signal/Noise: 0.0

Target • 2019fya • 23:15:16.062 • +19:02:29.832 Tel. Time: 01h00m

OS 1	WFM-NOAO	Observation
Tel. Time: 900 s	Instrument Mode: WFM-NOAO-N	Integration Time: 0 s
Repeat: 4 x	Telescope Overheads: 360 s	Instrument Overheads: 0 s
Total Tel. Time: 3600s		Signal/Noise: 0.0

Target • SN 2018imf • 12:42:41.389 • 13:15:54.889 Tel. Time: 01h00m

OS 1	WFM-NOAO	Observation
Tel. Time: 900 s	Instrument Mode: WFM-NOAO-N	Integration Time: 0 s
Repeat: 4 x	Telescope Overheads: 360 s	Instrument Overheads: 0 s

Total Tel. Time: 3600s | | Signal/Noise: 0.0

Target • SN 2020scb • 00:18:25.624 • 18:30:59.529 Tel. Time: 01h00m

OS 1	WFM-NOAO	Observation
Tel. Time: 900 s	Instrument Mode: WFM-NOAO-N	Integration Time: 0 s
Repeat: 4 x	Telescope Overheads: 360 s	Instrument Overheads: 0 s
Total Tel. Time: 3600s		Signal/Noise: 0.0

Target • SN 2020fzj • 20:15:42.935 • -06:18:59.878 Tel. Time: 01h00m

OS 1	WFM-NOAO	Observation
Tel. Time: 900 s	Instrument Mode: WFM-NOAO-N	Integration Time: 0 s
Repeat: 4 x	Telescope Overheads: 360 s	Instrument Overheads: 0 s
Total Tel. Time: 3600s		Signal/Noise: 0.0

Target • SN 2018fus • 21:02:31.199 • -05:37:30.069 Tel. Time: 01h00m

OS 1	WFM-NOAO	Observation
Tel. Time: 900 s	Instrument Mode: WFM-NOAO-N	Integration Time: 0 s
Repeat: 4 x	Telescope Overheads: 360 s	Instrument Overheads: 0 s
Total Tel. Time: 3600s		Signal/Noise: 0.0

Target • SN 2020aqb • 00:41:37.639 • -03:15:12.531 Tel. Time: 01h00m

OS 1	WFM-NOAO	Observation
Tel. Time: 900 s	Instrument Mode: WFM-NOAO-N	Integration Time: 0 s
Repeat: 4 x	Telescope Overheads: 360 s	Instrument Overheads: 0 s
Total Tel. Time: 3600s		Signal/Noise: 0.0

Target • SN 2019rn • 02:17:59.610 • 14:32:00.399 Tel. Time: 01h00m

OS 1	WFM-NOAO	Observation
Tel. Time: 900 s	Instrument Mode: WFM-NOAO-N	Integration Time: 0 s
Repeat: 4 x	Telescope Overheads: 360 s	Instrument Overheads: 0 s
Total Tel. Time: 3600s		Signal/Noise: 0.0

Target • SN 2018jq • 12:56:48.400 • 03:53:27.200 Tel. Time: 01h00m

OS 1	WFM-NOAO	Observation
Tel. Time: 900 s	Instrument Mode: WFM-NOAO-N	Integration Time: 0 s
Repeat: 4 x	Telescope Overheads: 360 s	Instrument Overheads: 0 s
Total Tel. Time: 3600s		Signal/Noise: 0.0

Target • SN 2020abcq • 08:44:31.499 • -20:20:47.360 Tel. Time: 01h00m

OS 1	WFM-NOAO	Observation
Tel. Time: 900 s	Instrument Mode: WFM-NOAO-N	Integration Time: 0 s
Repeat: 4 x	Telescope Overheads: 360 s	Instrument Overheads: 0 s
Total Tel. Time: 3600s		Signal/Noise: 0.0

Target • SN 2019dok • 13:46:51.756 • 16:16:53.731 Tel. Time: 01h00m

OS 1	WFM-NOAO	Observation
Tel. Time: 900 s	Instrument Mode: WFM-NOAO-N	Integration Time: 0 s
Repeat: 4 x	Telescope Overheads: 360 s	Instrument Overheads: 0 s
Total Tel. Time: 3600s		Signal/Noise: 0.0

Target • SN 2019nxk • 17:34:05.119 • -14:48:31.928 Tel. Time: 01h00m

OS 1	WFM-NOAO	Observation
Tel. Time: 900 s	Instrument Mode: WFM-NOAO-N	Integration Time: 0 s
Repeat: 4 x	Telescope Overheads: 360 s	Instrument Overheads: 0 s
Total Tel. Time: 3600s		Signal/Noise: 0.0